Virologica Sinica 38 (2023) 767–777

Contents lists available at ScienceDirect

Virologica Sinica

journal homepage: www.keaipublishing.com/en/journals/virologica-sinica
www.virosin.org

Research Article

Development of a novel virus-like particle-based vaccine for preventing tick-borne encephalitis virus infection

Jielin Tang [a,b,1], Muqing Fu [c,1], Chonghui Xu [b], Bao Xue [a,b], Anqi Zhou [d], Sijie Chen [d], He Zhao [b], Yuan Zhou [b], Jizheng Chen [a,b,e], Qi Yang [a,b,*], Xinwen Chen [a,b,e,*]

[a] Guangzhou National Laboratory, Guangzhou, 510005, China
[b] State Key Laboratory of Virology, Wuhan Institute of Virology, Center for Biosafety Mega-Science, Chinese Academy of Sciences, Wuhan, 430071, China
[c] Guangzhou Institutes of Biomedicine and Health, Chinese Academy of Sciences, Guangzhou, 510530, China
[d] GMU-GIBH Joint School of Life Sciences, Guangzhou Medical University, Guangzhou, 511436, China
[e] State Key Laboratory of Respiratory Disease, Guangzhou Medical University, Guangzhou, 511436, China

ARTICLE INFO

Keywords:
Tick-borne encephalitis virus (TBEV)
Virus-like particle (VLP)
Immunogenicity
Neutralization
Vaccine

ABSTRACT

Tick-borne encephalitis virus (TBEV) is an important tick-borne pathogen that poses as a serious public health concern. The coverage and immunogenicity of the currently available vaccines against TBEV are relatively low; therefore, it is crucial to develop novel and effective vaccines against TBEV. The present study describes a novel strategy for the assembly of virus-like particles (VLPs) by co-expressing the structural (core/prM/E) and non-structural (NS2B/NS3Pro) proteins of TBEV. The efficacy of the VLPs was subsequently evaluated in C57BL/6 mice, and the resultant IgG serum could neutralize both Far-Eastern and European subtypes of TBEV. These findings indicated that the VLP-based vaccine elicited the production of cross-subtype reactive antibodies. The VLPs provided protection to mice lacking the type I interferon receptor (*IFNAR*$^{-/-}$) against lethal TBEV challenge, with undetectable viral load in brain and intestinal tissues. Furthermore, the group that received the VLP vaccine did not exhibit significant pathological changes and the inflammatory factors were significantly suppressed compared to the control group. Immunization with the VLP vaccine induced the production of multiple-cytokine-producing antiviral CD4$^+$ T cells *in vivo*, including TNF-α^+, IL-2$^+$, and IFN-γ^+ T cells. Altogether, the findings suggest that noninfectious VLPs can serve as a potentially safe and effective vaccine candidate against diverse subtypes of TBEV.

1. Introduction

Tick-borne encephalitis virus (TBEV) is a zoonotic pathogen that causes mild or moderate febrile illness and fatal encephalitis with sequelae in humans (Bogovic and Strle, 2015; Taba et al., 2017). TBEV is endemic over a wide area of Europe and Asia and causes more than 13,000 cases annually worldwide, and the number of cases has increased over the past few decades owing to global climate change and expanding human habitats (Suss, 2008; Kunze, 2011). Based on sequences analysis of complete genome, there are three main TBEV subtypes: the Far Eastern (TBEV-FE), the European (TBEV-Eu), and the Siberian (TBEV-Sib) subtypes (Ruzek et al., 2019). The morbidity and mortality of TBE varies among these subtypes. TBEV-FE infections are the most severe, with a mortality rate of up to 40%. TBEV-Eu is associated with neurological sequelae in up to 10% of patients, with a 0.5%–2% mortality rate, while TBEV-Sib infections are prone to develop prolonged infections with a 2%–3% mortality rate (Pulkkinen et al., 2018).

TBEV belongs to the *Flavivirus* genus within the *Flaviviridae* family. Its genome is a single-stranded, positive-sense RNA with a length of approximately 11 kb nucleotides. The genome has one open reading frame (ORF) that encodes a single polyprotein which is co- and post-translationally cleaved by cellular and viral proteases into three structural proteins, including core (C), precursor-M (prM), and envelope (E) proteins, and seven non-structural proteins, namely, NS1, NS2A, NS2B, NS3, NS4A, NS4B, and NS5 (Fig. 1A) (Lindquist and Vapalahti, 2008; Füzik et al., 2018; Pulkkinen et al., 2018). Mature TBEV particles are approximately 50 nm in diameter and consist of a nucleocapsid surrounded by M and E proteins that are anchored within a lipid bilayer (Pulkkinen et al., 2018). The structural proteins mainly participate in the formation of viral particles, while the non-structural proteins play an

* Corresponding authors.
E-mail addresses: yang_qi@gzlab.ac.cn (Q. Yang), chen_xinwen@gzlab.ac.cn (X. Chen).
[1] Jielin Tang and Muqing Fu contributed equally to this work.

https://doi.org/10.1016/j.virs.2023.06.003
Received 12 March 2023; Accepted 12 June 2023
Available online 14 June 2023

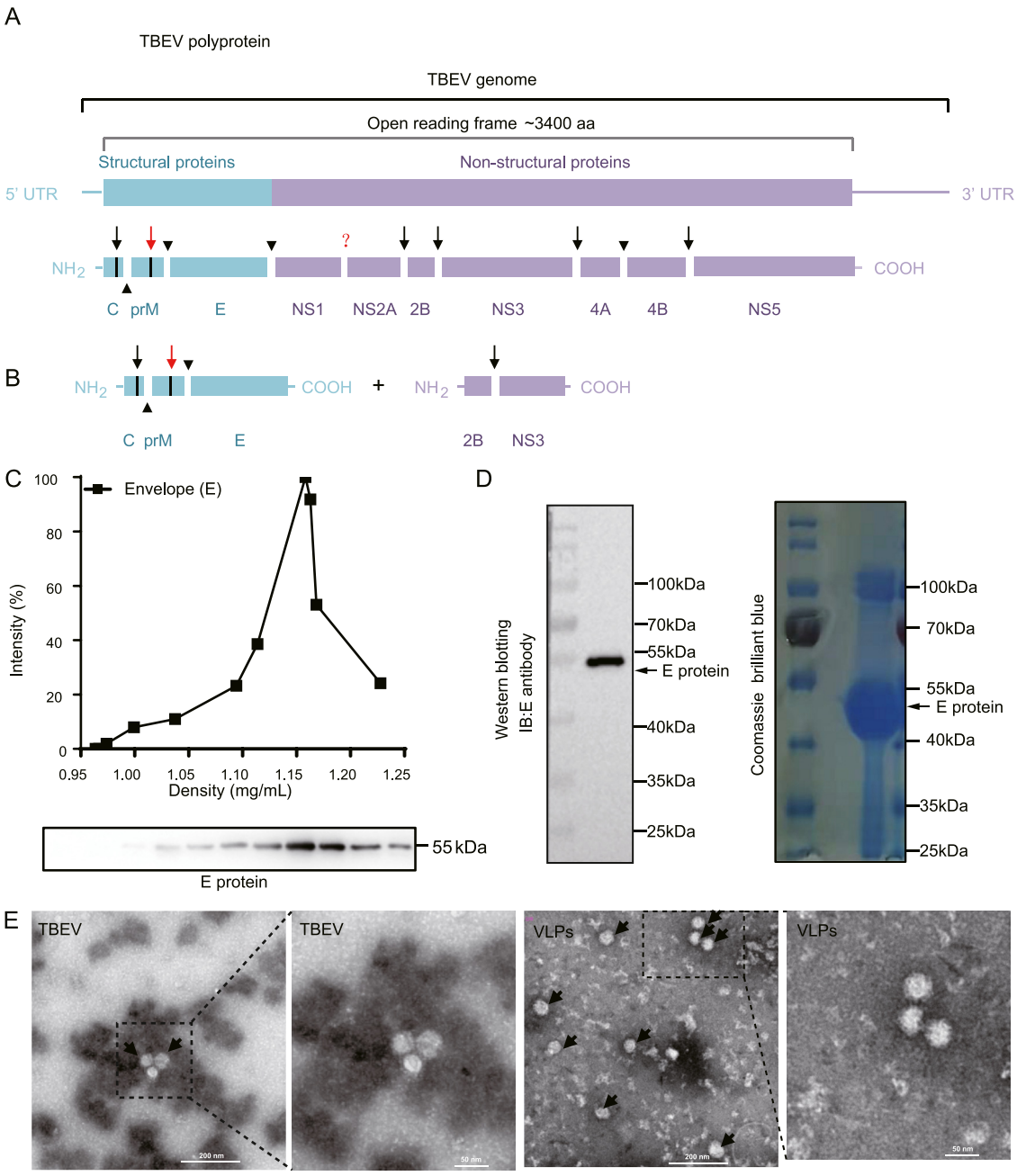

Fig. 1. Construction of the candidate TBE VLP vaccine. **A** Schematic representation of the single ORF in the TBEV genome that translates into a polyprotein comprising the structural and non-structural proteins. The structural proteins are depicted in shades of blue while the non-structural proteins are represented in shades of orange. The complex formed by the viral NS3 protease and the NS2B co-factor self-cleaves before cleaving the C protein. The host signalase protein is also involved in polyprotein maturation. The furin protein of the host finally cleaves the pr portion from the M protein to release the E protein fusion peptide. The black arrows indicate viral serine protease cleavage sites, the triangles indicate host signal peptidase cleavage sites, the interrogation mark indicates the cleavage site of an unknown host protease, and the red arrow indicates a furin cleavage site. **B** Schematic depicting the construction of the VLP-based vaccine candidate. The strategy used for assembling the VLP was based on the co-expression of the structural proteins (C/prM/E) and non-structural proteins (NS2B/NS3Pro) of TBEV. The viral NS3 protein was truncated and only contained the N-terminal protease domain, which was placed in a single transcription unit with the NS2B co-factor. **C** Buoyant density-gradient analysis of the constructed VLPs. The plasmids were transfected into Expi293 cells, and the supernatants were collected after four days. The VLPs were purified by density gradient centrifugation. The expression of the viral E protein was confirmed by Western blotting. **D** Analysis of the purified VLPs by Coomassie blue staining and Western blotting. **E** TEM images of the wild type TBEV and the VLPs. The results represent the mean ± standard deviation (SD) of data obtained from at least three independent experiments.

important role in viral replication and evading the innate immune response (Werme et al., 2008; Yang et al., 2020). The E protein is a viral surface glycoprotein that mediates receptor binding and membrane fusion, and plays an important role in inducing protective immunity and vaccine development.

Despite the health threat posed by TBEV, no licensed antiviral drugs against TBEV exist at present, and current strategies for the treatment of TBEV are only supportive in practice (Studahl et al., 2013; Taba et al., 2017). Therefore, active immunization is the most important protective measure against TBEV infection. Despite the good tolerability, the safety

and field efficacy of the currently available inactivated vaccines against TBEV have certain disadvantages (Loew-Baselli et al., 2006; Demicheli et al., 2009), such as time-consuming vaccination schedules and incomplete protection, particularly among older adults. The efficient induction of virus-specific memory B and T cell responses is pivotal for providing durable protective immunity and preventing vaccination breakthrough infections in TBEV vaccinees (Kubinski et al., 2020). Therefore, the exploration and development of novel vaccination strategies may aid in overcoming some limitations of currently licensed TBEV vaccines.

Considerable efforts have been made in recent years towards developing vaccines based on TBEV particles containing different forms of the E protein generated using recombinant subviral particles. The efficacy of recombinant subviral particles is similar to inactivated vaccine in terms of antibody induction and protection against viral challenge, while all soluble forms of the E protein have considerably lower immunogenicity (Heinz et al., 1995). One study demonstrated that the vaccination of mice with a recombinant vaccinia virus encoding the prM and E proteins provided robust protection following challenge infection with TBEV. However, according to the dose of vaccination, the titers of the neutralizing antibody (NAb) were relatively low and did not increase considerably (Holzer et al., 1999). It is therefore necessary to develop improved vaccines with stronger immunogenicity.

Virus-like particles (VLPs) are highly immunogenic and completely devoid of viral genetic material that is necessary for replication. VLP-based vaccines are therefore non-infectious and safer than live-attenuated or whole-inactivated vaccines (Chen and Lai, 2013). Notably, the small size of VLPs allows rapid diffusion through lymph nodes and facilitates antigen presentation for the induction of B and T cells. VLPs have been employed for investigating the function, morphogenesis, and structure of proteins, and for generating vaccines against flaviviruses (Liu et al., 2014; Taylor et al., 2016; Yamaji and Konishi, 2016; Boigard et al., 2017), which can be produced in yeast, plant, insect, or mammalian cells (Liu et al., 2005; Urakami et al., 2017; Metz et al., 2018). Incorporating the C protein into the VLPs can increase the numbers of epitopes, as demonstrated on Zika VLPs (Garg et al., 2017; Lin et al., 2018). The NS3 protein functions as a viral serine protease (with NS2B as a co-factor), RNA helicase, and nucleoside triphosphatase, and plays a central role in viral replication and protein processing (Lobigs, 1993; Stocks and Lobigs, 1998). Recent studies have demonstrated that Zika VLPs containing the full-length C, prM, and E proteins along with the viral NS2B/NS3 protease complex, generate higher Zika VLP titers and antibody concentrations (Malogolovkin et al., 2023). A similar study revealed that the co-expression of the structural proteins (C/prM/E) and non-structural (NS2B/NS3) proteins of the Zika virus (ZIKV) increased the self-assembly of C and prM proteins into particles closely resembling ZIKV, and proved to be effective as live-attenuated or whole-inactivated vaccines (Boigard et al., 2017).

In this study, we used a similar strategy to design and evaluate the VLP vaccine against TBEV. Our results showed that the VLPs efficiently induced E-specific humoral immune responses in mice. Immunization with VLPs induced multiple $CD4^+$ T cell response and prevented mice from a lethal TBEV challenge. These results suggest that VLPs represent a promising vaccine candidate for the prevention of TBEV infection.

2. Materials and methods

2.1. Virus and cell lines

The TBEV-FE (WH2012, KJ755186) and TBEV-Eu (Neudoerfl, U27495) subtypes of TBEV were obtained from the National Virus Resource Center of China, and propagated and titrated in BHK-21 cell lines as previously described (Li et al., 2021). BHK-21 cells (ATCC® CCL-10) were cultured in Dulbecco's modified Eagle's medium (DMEM, Gibco) supplemented with 10% fetal bovine serum (FBS, Gibco), 100 U/mL penicillin and 100 μg/mL streptomycin (Invitrogen) at 37 °C in an atmosphere of 5% CO_2. Expi293F cells (Thermo Fisher, A14527) were maintained in Expi293F culture medium (Thermo Fisher, A1435101) and incubated in an orbital incubator shaker at 37 °C in an atmosphere of 5% CO_2.

2.2. Plasmid construction and molecular cloning

The sequences encoding the structural (C/prM/E) or non-structural (NS2B/NS3Pro) proteins of TBEV were chemically synthesized by TSINGKE Biological Technology according to codon optimization, and derived from the genome of the WH2012 strain of TBEV. The nucleotide sequence of these plasmids was showed in Supplementary Table S1. The synthesized DNA fragments were subcloned into the pcDNA3.1(−) plasmid at the *Xho*I/*Kpn*I restriction sites, followed by transformation into chemically competent DH5α cells. The resulting plasmids were purified using the EndoFree Plasmid Maxi Kit (Qiagen, MD).

2.3. Production and purification of VLPs

Expi293 cells were diluted to a density of 1.5×10^6 cells/mL before transfection with pcDNA3.1-NS2B/NS3Pro and pcDNA3.1-C/prM/E at a ratio of 1:2, then the cells were cultivated at 37 °C in an atmosphere of 5% CO_2, with agitation at 150 rpm. For the production of VLPs, the plasmids (480 μg) were added to polyethylenimine hydrochloride (1350 μg; Polysciences) in 10 mL of Expi293 medium and incubated for 10 min, the mixture was then added to 470 mL of cell solution. The transfected cells were harvested at 4 days post-transfection and the supernatant was collected by two successive centrifugation steps at 400 ×*g* for 10 min at 4 °C, then 10,000 ×*g* for 10 min at 4 °C. The proteins in the supernatant were precipitated using 8% (*wt/vol*) polyethylene glycol 8000 and incubated overnight at 4 °C.

For purification of the VLPs, protein pellets were collected by centrifugation at 10,000 ×*g* for 1 h at 4 °C and loaded onto a 20% (*wt/vol*) sucrose cushion in TNE buffer (10 mmol/L Tris-HCl, pH 8.0, 120 mmol/L NaCl, and 1 mmol/L EDTA), followed by ultracentrifugation at 87,000 ×*g* for 2 h at 4 °C. The pellet was re-suspended in TNE buffer, and the VLPs were subsequently purified by ultracentrifugation through a linear sucrose density gradient (20%–60%, [*wt/vol*]) at 250,000 ×*g* for 4 h at 4 °C. Selected fractions were further purified and concentrated using an Amicon Ultra Centrifugal Filter Unit (Millipore, MA, USA).

2.4. Purification of TBEV E protein and generation of anti-TBEV polyclonal E antibody

The coding sequence for residues 1–401 aa in the ectodomain of the E protein (sE) of the WH2012 strain of TBEV were codon optimized and cloned into a pET21a vector with a C-terminal His_{10}-tag. The sE proteins were then expressed in *Rosetta* (DE3) as inclusion bodies and subsequently refolded *in vitro* as previously described (Dai et al., 2016). The refolded proteins were concentrated using an Amicon 400 concentrator with a 30-kDa cutoff membrane. The sE proteins were further purified by gel filtration using an AKTA Pure System with a HiLoad 16/60 Superdex 200 PG column (GE Healthcare).

Briefly, C57BL/6 mice were immunized with the purified TBEV E protein by three intramuscular injections. Anti-TBEV E antibody was isolated from the sera of the immunized C57BL/6 mice. The characterization of the antibody was subsequently verified by Western blotting and immunofluorescence (IF).

2.5. Western blotting

The fractions obtained by centrifugation were subsequently separated by electrophoresis. Briefly, 10 μL of each sample was resolved by sodium dodecyl sulphate-polyacrylamide gel electrophoresis (SDS-PAGE), and the blots were transferred to a nitrocellulose membrane. The membranes were blocked by incubating with 5% non-fat milk in TBST (10 mmol/L Tris-HCl, pH 7.4, 130 mmol/L NaCl, 2.7 mmol/L KCl, and 0.1% Tween-20) for

1 h at room temperature followed by overnight incubation at 4 °C using an anti-TBEV mouse polyclonal E antibody. The membranes were washed thrice with TBST and subsequently incubated for 1 h with a secondary antibody. The membranes were finally washed with TBST and the images were captured using a FluorChemHD2 system.

2.6. Negative-stain electron microscopy

For electron microscopy, 10 μL of each sample was placed on the grid and incubated for 1 min, following which excess sample was removed by touching the edge of the grid to a filter paper. Negative staining was applied using 10 μL of 2% phosphotungstic acid (PTA; pH 7.0) and incubated for 3 min. Excess stain was gently removed with a filter paper. The grid was dried at room temperature, and transmission electron microscopy (TEM) images were captured using a 200 kV Tecnai electron microscope.

2.7. Mice infection experiments

Eight-week-old male C57BL/6 mice were used for the immunization and viral neutralization experiments. The mice (n = 5 per group) were immunized by twice intramuscular injections with PBS or 10 μg of VLPs. The dosage of VLPs used in this study were referenced as previously described (Vang et al., 2021; Zhao et al., 2021; Yang et al., 2022). Blood samples were collected from the orbital sinus at indicated time points, and transferred to blood collection tubes. Serum was separated by centrifugation at 3000×*g* for 10 min at room temperature (~25 °C) and stored at −80 °C until further use.

IFNAR$^{-/-}$ mice, with a C57BL/6 background, were obtained from the Suzhou Institute of Biomedical Engineering and Technology, CAS. These mice lack the receptor for type I interferons. Six to eight-week-old male *IFNAR*$^{-/-}$ mice were used for immunization and challenge experiments (Phanthanawiboon et al., 2016). The mice (n = 10 per group) were immunized with PBS or 10 μg of VLPs as mentioned above. They were then challenged subcutaneously with a lethal dose of the WH2012 strain of TBEV (3.2×10^6 PFU) at 6 weeks post-second injection of either PBS or VLPs. The body weights and survival rates of the mice were monitored for 14 days following challenge. Blood samples and tissues of the mice were collected at the indicated time points, and viral quantitation was performed using the $TCID_{50}$ assay. All the experiments were repeated independently at least once.

2.8. Determination of antibody titers

The level of TBEV-specific IgG antibody in the immunized mice was determined by enzyme-linked immunosorbent assay (ELISA). Briefly, 96-well plates were coated with purified TBEV-E protein and blocked with PBS containing 5% skim milk. Sera from the immunized mice were added to the coated wells at a dilution of 1:50 and incubated. This was followed by incubation with a horseradish peroxidase (HRP)-conjugated goat anti-mouse IgG secondary antibody. A two-component 3,3′,5,5′-tetramethylbenzidine (TMB) color development kit (Beyotime Bio-technology) was used for detecting the bound antibody. Following the addition of 1 mol/L H_2SO_4 stop solution, the optical density was measured at a wavelength of 450 nm using a multimode microplate reader (Varioskan Flash; Thermo Fisher).

2.9. Evaluation of NAb titers

The neutralization of E antibody was evaluated. The TBEV-FE strain (MOI = 0.1) was preincubated with the E antibody diluted at a 5-fold dilution, from a starting dilution of 1:10, for 1 h at 37 °C. The mixtures were then added to a monolayer of BHK-21 cells at a density of 8×10^4/ well before seeding into 24-well plates. The cells were further incubated at 37 °C in an atmosphere of 5% CO_2 for 3 days. The relative intracellular viral RNA was quantified by qRT-PCR. Based on the results of E antibody neutralization assay, the serum samples of the vaccinated mice were suitably diluted to a ratio of 1:50 for subsequent experiments.

The serum samples were heat inactivated for 30 min at 56 °C. 2×10^4 BHK-21 cells were seeded in a 96-well plate for 20 h. The TBEV-FE strain WH2012 (MOI = 0.1) or TBEV-Eu strain Neudoerfl (MOI = 0.1) was preincubated with the serum samples diluted with the sera obtained from the vaccinated mice at a dilution of 1:50, for 1 h at 37 °C, and then 150 μL mixtures were inoculated onto monolayer BHK-21 cells. Three days after inoculation, cytopathic effect (CPE) was quantified. The inhibition of mice sera was calculated based on the CPE rates of TBEV.

2.10. $TCID_{50}$ assay

TBEV titer was determined by 50% tissue culture infective dose (TCID50) assay with 10-fold serial dilutions in BHK-21 cells as described (Yang et al., 2021; Tang et al., 2023). Briefly, BHK-21 cells were seeded in 96-well plates at a density of 2×10^4/well and inoculated with serially diluted serum samples and tissue homogenate. Eight replicates were set for each dilution. The wells with CPE were counted on day 3 post-inoculation, and the $TCID_{50}$ was calculated by the Reed-Muench formula.

2.11. Histological analyses

The samples of the brain and small intestinal tissues of the vaccinated mice following challenge were fixed with 4% paraformaldehyde, embedded in paraffin, and sliced into 3.5-mm-thick sections. The fixed tissues were subjected to hematoxylin-eosin (H&E) staining and immunofluorescence assays. For the immunofluorescence studies, the tissue sections were treated with the TBEV E antibody (1:500) and subsequently washed with PBS. The sections were then dried, and the tissues were incubated with 488-conjugated goat-anti-mouse secondary antibody (Invitrogen) at a dilution of 1:500. Slides were washed with PBS and stained with DAPI (Invitrogen) at a dilution of 1:1000. Images were finally captured using a Pannoramic MIDI system (3DHISTECH, Budapest) and a FV1200 confocal microscope (Olympus). Clinical scores were used to assess the severity of brain or intestinal injury. Detailed histological assessments of brain and intestinal tissues were provided in Supplementary Table S2 and Table S3.

2.12. RNA extraction and qRT-PCR

Total cellular RNA was extracted with Trizol reagent according to the manufacturer's protocols (Invitrogen, USA). Specific gene transcripts were quantified by one-step real-time qRT-PCR with specific primers and the HiScript II One Step qRT-PCR SYBR Green Kit (Vazyme) on the Applied Biosystems QuantStudio 6 Flex. The data were normalized to the expression of the β-actin for each individual sample. The relative expression level was calculated by $2^{-\Delta\Delta Ct}$ method. The primer sequences for WH2012 were designed as follows: Forward: 5′-CACAACCTGGAGTGCTCG-3’; Reverse: 5′-ACCATGTTCGGCCTTATC-3’.

2.13. RNA sequencing (RNA-seq)

Brain tissues of the mice in the PBS and VLP groups were harvested at 7 days post-infection (dpi). Total RNA was extracted with Trizol reagent. Then the RNA-Seq was performed by Beijing Qingke Biotechnology Co., Ltd. Briefly, sequencing libraries were generated for Illumina®. Library acquisition was obtained by sequencing on an Illumina HiSeq 4000 platform, yielding 150 bp paired-end reads.

2.14. Flow cytometric analyses

C57BL/6 mice were immunized with either PBS or 10 μg of VLP for both prime and boost immunization. Splenocytes were isolated from the spleens of immunized mice after 14 days of boost immunization to

analyze cytokines induction following immunization. Briefly, the isolated splenocytes were stimulated by incubation with Phorbol myristate acetate (PMA) plus ionomycin (IONO) or E antigens at 37 °C for 6 h in the presence of GolgiPlug (BD Biosciences). The treated cells were then washed with a staining buffer (2% FBS in PBS) and stained by incubating with an FITC anti-mouse CD4 antibody (BioLegend) for 30 min at 4 °C. The cells were washed and subsequently fixed and permeabilized with BD Fix/Perm buffer at 4 °C for 20 min. The cells were then stained with the PE anti-mouse IFN-γ^+ antibody (BioLegend), pacific blue™ anti-mouse IL-2^+ antibody, and the APC/Cyanine7 anti-mouse TNF-α^+ antibody (BioLegend). Finally, the cells were washed and analyzed by flow cytometry.

2.15. Statistical analyses

Statistical analyses were performed using GraphPad Prism 6 software. Significant differences between groups were determined by one-way analysis of variance (ANOVA) and two-tailed Student's *t*-tests. Differences were considered to be statistically significant at $*P < 0.05$, $**P < 0.01$, and $***P < 0.001$.

3. Results

3.1. Generation of TBE VLPs

To produce recombinant VLPs, structural proteins (C/prM/E) were co-expressed with non-structural proteins (NS2B/NS3Pro) in Expi293F cells (Fig. 1B). The VLPs were harvested from the cell culture supernatant and purified as described previously (Boigard et al., 2017). Following buoyant density-gradient sedimentation, the main components of purified particles (E protein) were analyzed by SDS-PAGE, as depicted in Fig. 1C. The TBEV E protein exhibited the highest density of about 1.15 g/mL. Coomassie blue staining revealed that the E protein was the predominant component in the prepared VLPs, and the identity of the E protein was further verified by Western blotting (Fig. 1D). The result of negative-stain TEM revealed that the VLPs were homogeneous spherical structures with a diameter of approximately 40–50 nm (Fig. 1E). Their morphological characteristics were similar to the wild type TBEV particles (Fig. 1E), which were consistent with previous study (Füzik et al., 2018; Pulkkinen et al., 2018).

3.2. VLPs induced robust NAb responses

The C57BL/6 mice received twice intramuscular injections of 10 μg VLPs over a four-week interval (Fig. 2A). The neutralizing ability of the sera was evaluated two weeks post-boost injection. A clear correlation between serum dilution and neutralizing effect was observed, with samples diluted up to a factor of 1:250 maintaining robust TBEV neutralizing ability (Fig. 2B).

Total serum IgG response in vaccinated mice was determined by ELISA, by using the purified E protein of TBEV. The TBEV E protein antigen and the anti-E antibody were produced in our laboratory and characterized as depicted in Supplementary Fig. S1. The results of ELISA demonstrated that vaccination with the VLPs stimulated a high total serum IgG response, and the prime antibody response increased by 2.5-fold following boost immunization (Fig. 2C). Additionally, the antibodies elicited by the VLPs significantly neutralized both TBEV-FE and TBEV-Eu infections in BHK-21 cells, with inhibition rates reaching up to 90% (Fig. 2D). Altogether, these findings suggested that the VLPs exhibited superior immunogenicity and induced high levels of humoral immunity (IgG and NAb) against different subtypes of TBEV.

3.3. VLPs protected mice against TBEV challenge

In order to evaluate the immunoprotective efficacy of the VLPs, VLP-immunized *IFNAR*$^{-/-}$ mice were challenged with a lethal dose (3.2×10^6 PFU) of the WH2012 strain of TBEV by intramuscular injection after two weeks post-boost immunization with 10 μg VLPs (Fig. 3A). Mouse body weight and physical appearance were monitored for two weeks. We observed that the body weight of infected mice was decreased

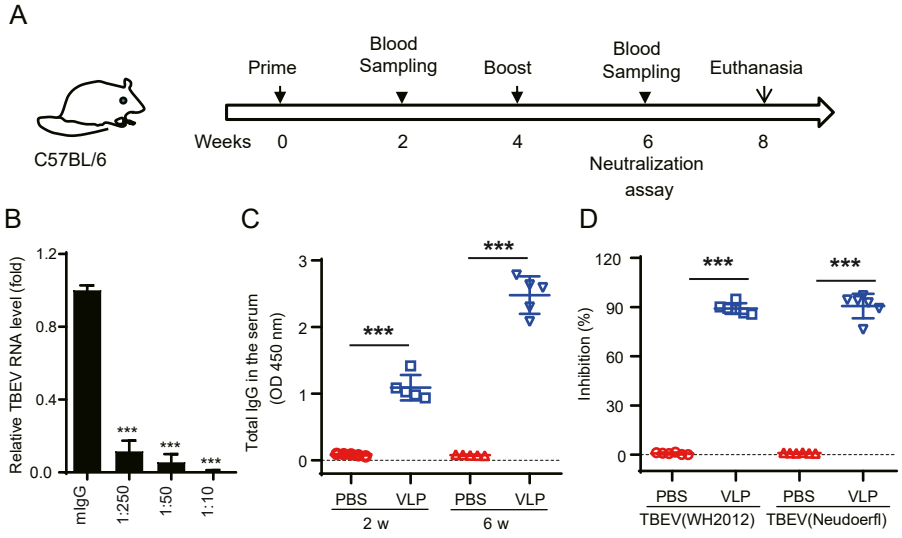

Fig. 2. Antigen-specific antibody responses induced by immunization with the VLPs. Eight-week-old C57BL/6 mice (n = 5 per group) were immunized by twice intramuscular injections with PBS or VLPs (10 μg) in the D0 and D28 immunization programs, respectively. **A** Time course of the vaccination and neutralization assays. **B** NAb titers of E protein antibody which was isolated from E protein immunized mice sera at different dilution ratio were evaluated by preincubation with the TBEV-FE (MOI = 0.1) for 1 h at 37 °C before the addition of BHK-21 cells. Three days after incubation, the cellular viral RNA level was quantified by qRT-PCR. **C** The antibody response in the sera of the VLPs vaccinated mice was detected by virion-based IgG ELISA at the indicated time points. **D** The NAb titers in the sera of the VLP immunized mice were evaluated by preincubation with the TBEV-FE (WH2012, MOI = 0.1) or the TBEV-Eu (Neudoerfl, MOI = 0.1) subtype for 1 h at 37 °C before the addition of BHK-21 cells. CPE was counted on 3 dpi and the inhibition of mice sera was calculated from TBEV's CPE rates. The results represent data obtained from three independent experiments. Each data point represents the mean ± standard deviation (SD) of the values from five mice per group. $***P < 0.001$ (Student's *t*-test).

continuously, with a rapid decrease observed at 3 dpi (Fig. 3B). Moreover, the infected mice displayed some abnormal behaviors, such as listlessness, circling and freezing, and all the infected mice died within 8 dpi (Fig. 3C). In contrast, immunized mice survived the challenge, and their weights did not decrease significantly (Fig. 3B and C).

Viremia was determined by $TCID_{50}$ assays at 3 dpi, and brain and small intestinal tissues were obtained at 7 dpi. The viremia of the control group was notably high (7.9×10^4 $TCID_{50}$/mL) (Fig. 3D), with average values in the brain and intestinal tissues reaching 1.0×10^7 and 5.0×10^5 $TCID_{50}$/mL, respectively (Fig. 3E and F). In contrast, the mice that had been immunized with the VLPs did not exhibit any neurological symptoms and the viral loads in the serum samples, brain, and intestinal tissues were negligible or undetectable (Fig. 3D–F). Altogether, these findings confirmed that VLPs conferred complete protection against TBEV infection.

3.4. Pathological changes in vaccinated mice following TBEV challenge

Pathological changes in brain and intestinal tissues were detected by H&E staining at 7 dpi. Histological analysis of brain tissue sections revealed that the control group exhibited neuronal necrosis, degeneration, and disruption of normal cytoarchitecture, as depicted by the black arrow in Fig. 4A. Analysis of the intestinal tissues revealed moderate abnormalities, including the presence of villi with loose and irregular structures and abscission of the intestinal mucosa (Fig. 4B). The results of histological analysis also revealed the massive infiltration of inflammatory cells in the mucosal layer, which is depicted by the red arrow in Fig. 4B. In contrast, there were no obvious lesions in the brain and intestinal tissues of the immunized mice, and the viral antigen was detected by immunohistochemistry (Fig. 4A and B). Consistent with the pathological observations, no viral antigen was identified in VLP-vaccinated group. Histological scores were assessed and statistically analyzed as shown in Fig. 4C, and the score of the VLP group was lower than that of the control group.

It has reported that the increased levels of various cytokines in the serum and brain tissues of TBEV-infected mice are generally determined in a time-dependent manner (Pokorna Formanova et al., 2019). The induction of pro-inflammatory cytokines in the brain tissues was therefore determined at 7 dpi by RNA-seq. The findings revealed significant upregulation of certain key inflammatory cytokines, including CXCL10, RANTES, and MCP-1, in non-immunized mice. However, vaccination with the VLPs protected mice from TBEV challenge, with few or no pro-inflammatory cytokines detected in the vaccinated mice, which could partially explain the alleviated brain pathology (Fig. 4D). Altogether, these results demonstrated that vaccination with the VLPs did not induce any pathogenic alterations, and few or no inflammatory cytokines were activated and recruited.

3.5. $CD4^+$ T cell responses in VLP-vaccinated mice

To determine the ability of VLPs to induce $CD4^+$ T cell immune responses after VLPs vaccination following the prime-boost immunization strategy, the mice in the immunized and non-immunized groups were sacrificed after two weeks post-boost immunization. Splenocytes were isolated and assayed for cytokines production. The $CD4^+$ T cells were assayed for the expression of TNF-α^+, IL-2^+, and IFN-γ^+ by flow cytometry

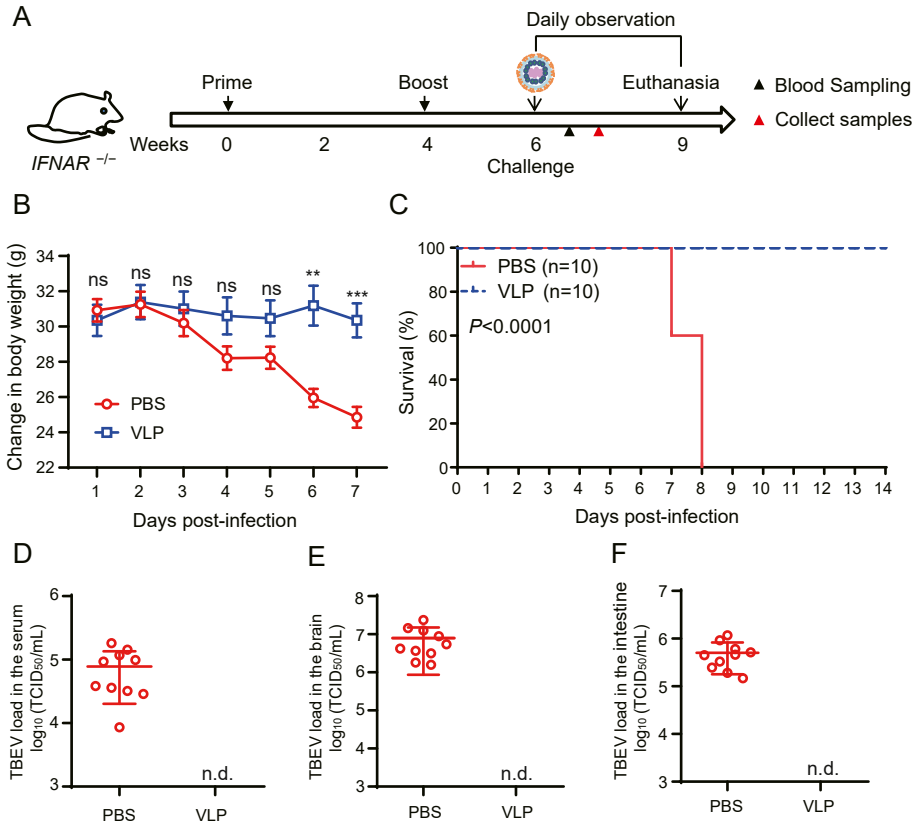

Fig. 3. VLPs protected against TBEV challenge in mice. Eight-week-old male *IFNAR*$^{-/-}$ mice (n = 10 per group) were immunized by twice intramuscular injections with PBS or VLPs (10 μg) in the D0 and D28 immunization programs, respectively. The mice were challenged with a lethal dose of TBEV (PFU = 3.2×10^6) at 6 weeks, which was followed by a 2-week monitoring period. **A** Time course of the vaccination and challenge. **B** The body weights of the mice were recorded for 7 dpi, and (**C**) the survival rates were determined for 14 dpi. **D** Viremia was quantified from the sera at 3 dpi. The viral load in the **(E)** brain and **(F)** intestinal tissues was quantified at 7 dpi (n = 6). The results represent the data obtained from three independent experiments. Each data point represents the mean ± standard deviation (SD) of the values from five mice per group; n.d., not detected. $^{**}P < 0.01$; $^{***}P < 0.001$; ns: not significant (Student's *t*-test).

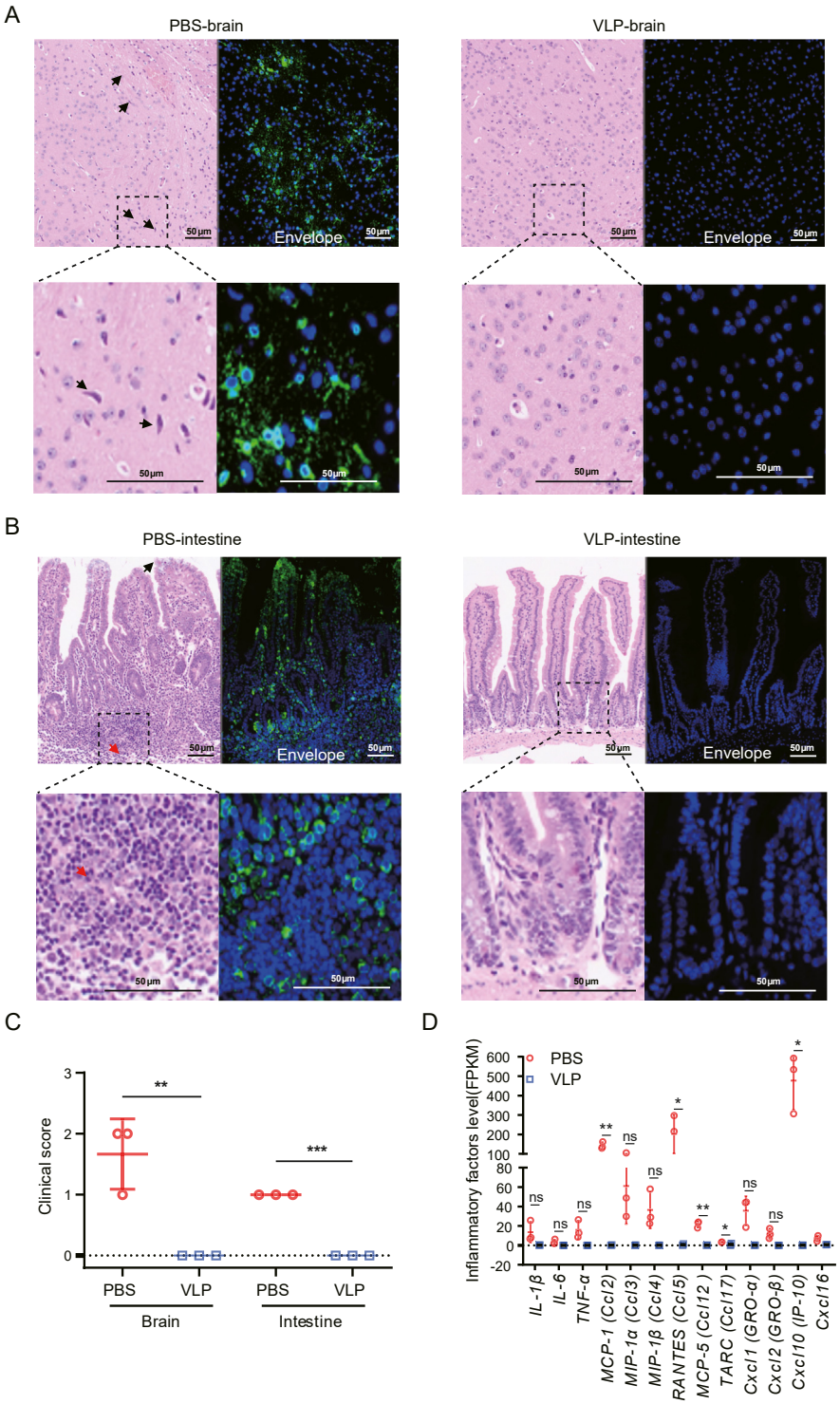

Fig. 4. Pathological changes in the brain and intestinal tissues of mice following TBEV infection. The assessment of pathological changes and antigens in the (**A**) brain and (**B**) intestinal tissues of mice at 7 dpi by using H&E staining and IF studies. Neuronal degeneration in the control group is depicted by the black arrow, and the red arrow indicates the infiltration of inflammatory cells. The viral antigens were detected in the same tissue sections using an anti-E polyclonal antibody (green). Magnification: 30× , scale bar: 50 μm. **C** Clinical scores determined from the organs of challenged mice at 7 dpi. The histological scoring criteria of brain and intestine were shown in Supplementary Table S1 and Table S2, respectively. **D** Downregulation of cytokines and chemokines in the brain tissues of immunized mice. The brain tissues of the mice in the control and VLP groups were harvested at 7 dpi, and the multiple cytokines and chemokines were measured by RNA-seq. The results represent the data obtained from at least three independent experiments. n = 3, $^{*}P < 0.05$; $^{**}P < 0.01$; ns: not significant (Student's *t*-test).

following stimulation with PMA/ionomycin or E antigens. Unstimulated cells were used as the negative control. The results demonstrated no significant differences in the percentage of TNF-α^+, IL-2^+, and IFN-γ^+ $CD4^+$ T cells between the control and VLP groups in the absence of stimulation (Fig. 5A and B). However, stimulation with PMA/ionomycin and E antigens induced higher IFN-γ^+, IL-2^+, and TNF-α^+ $CD4^+$ T cell responses in the VLP group. Altogether, these findings suggested that immunization with the VLPs could induce T cell-mediated immunity in mice.

4. Discussion

TBEV infection causes a serious neurological condition in human; however, there are no specific antiviral treatments for TBEV at present. Traditional methods such as formaldehyde-inactivated vaccines or recombinant vaccinia virus-based TBEV vaccines provide incomplete protection against TBEV or have relatively low immunogenicity. These challenges can be addressed by VLP-based vaccines, which are known to be safe, generate an effective immune response, and can readily be scaled up for cost-effective production (Jeong and Seong, 2017). The VLPs of TBEV generated in this study induced higher NAb titers and $CD4^+$ T cell immune response in the immunized mice, and protected *IFNAR*$^{-/-}$ mice against a lethal TBEV challenge. The study describes a promising strategy for improving immunity against TBEV infection which could serve as a potential vaccination approach for combating TBEV.

This study describes a novel strategy for generating VLPs by co-expressing the C/prM/E proteins and the NS2B/NS3Pro plasmids of TBEV in Expi293 cells. The purity and composition of the purified VLPs were assessed by Coomassie blue staining and Western blotting. The presence of the E protein was verified by Western blotting and exactly correlated with the E protein visualized in Coomassie blue staining. The M protein could not be clearly visualized in the gel following Coomassie blue staining, which was possibly attributed to the small size and low

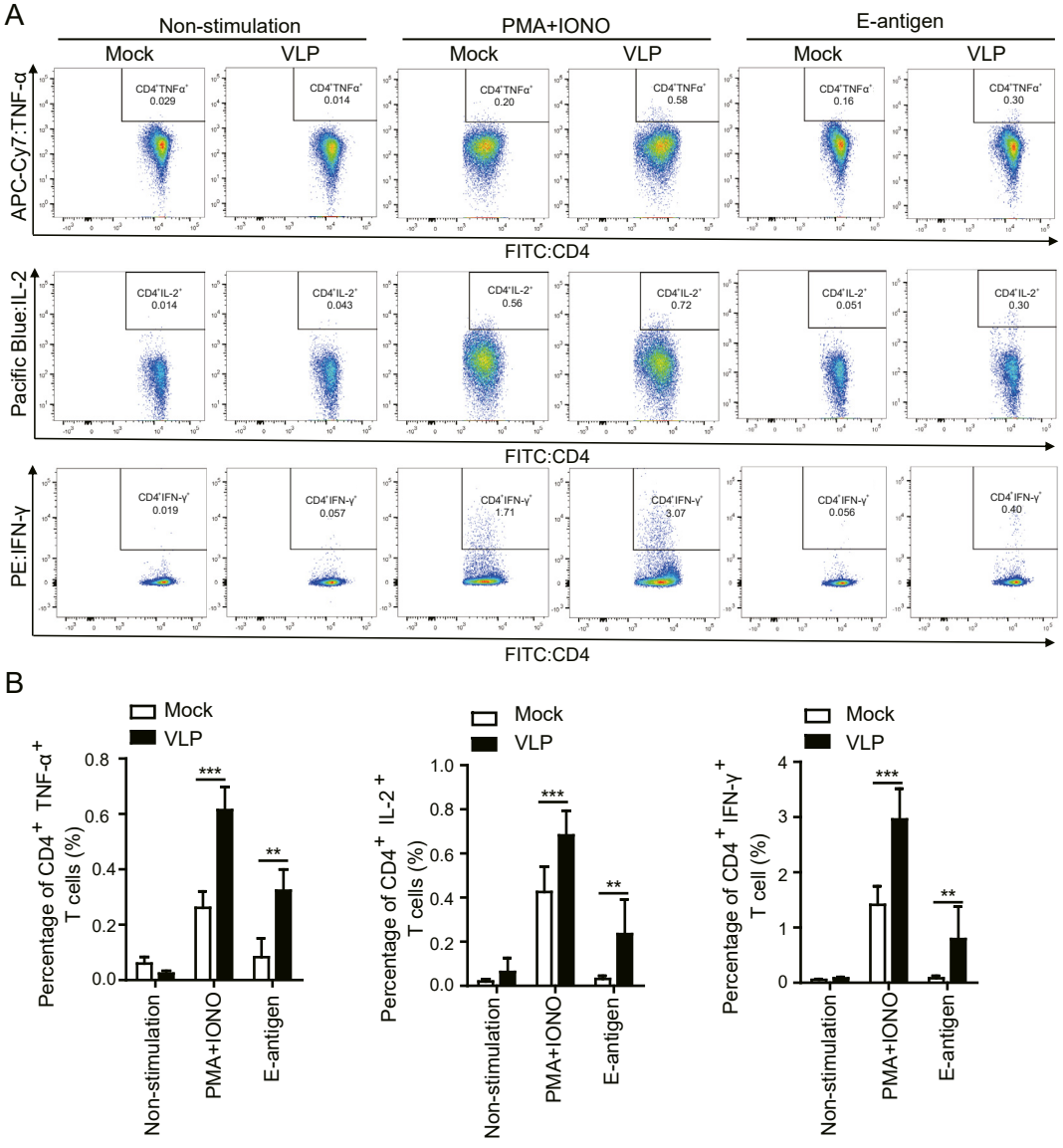

Fig. 5. $CD4^+$ T cell responses in VLP vaccinated mice. C57BL/6 mice were immunized with PBS or VLPs following prime and boost immunization. The splenocytes obtained from the mice in the control and VLP groups after 14 days of boost immunization were stimulated for 6 h with PMA/ionomycin or E antigen and the cells were analyzed by flow cytometry for determining the intracellular production of TNF-α^+, IL-2^+, and IFN-γ^+ $CD4^+$ T cells. **A** Representative flow cytometry contour plots of TNF-α^+, IL-2^+, and IFN-γ^+ $CD4^+$ T cells. The $CD4^+$ T cells were gated, and the percentage of TNF-α^+, IL-2^+, and IFN-γ^+ $CD4^+$ cells are indicated in the top right corner. **B** Summary of the cumulative data depicting the percentage of $CD4^+$ T cells with different cytokine production profiles in mice treated with PBS or the VLPs. The unstimulated splenocytes were used as the negative control. The results represent the mean ± SD of data obtained from five mice per group. $^{**}P < 0.01$; $^{***}P < 0.001$ (Student's *t*-test).

concentration. The M and C proteins in the purified VLPs were not detected by Western blotting owing to the absence of the corresponding antibodies. Nevertheless, a study aimed at assembling Zika VLPs using the same protocol reported that the major structural (E and M) proteins can be identified by Western blotting using specific antibodies (Boigard et al., 2017). Another study used a bicistronic vector expressing the C/prM/E and NS2B/NS3 proteins of ZIKV to generate C/prM/E VLPs could induce a superior NAb response compared to only expressing prM/E VLPs, and the C-specific antibodies were detected in the immunized mice (Garg et al., 2019). Additionally, the TBE VLPs purified in our study exhibited homogeneous spherical structures with a diameter of approximately 40–50 nm, similar in size, morphology, and antigenic composition to wild type TBEV (Füzik et al., 2018). In contrast, recombinant TBEV subviral particles which only contained prM-E were observed about 30 nm in diameter (Liu et al., 2005).

It is known that TBEV NAbs primarily target epitopes located in the E protein. However, immunization with various soluble forms of whole dimeric or membrane anchor-free TBEV E proteins fail to induce the production of viral NAbs and are incapable of inducing the necessary immunogenicity in mice (Heinz et al., 1995). Similarly, DNA vaccines driving the intracellular expression of whole or truncated TBEV E proteins, or the secretion of TBEV E dimers, fail to induce the production of viral NAbs and provide robust protection against TBEV (Aberle et al., 1999). The correct conformation of E protein determines the high-level immunogenicity of vaccines. In our study, specific antibodies elicited by the VLPs were sufficient to provide protection against the different subtypes of TBEV. The findings were consistent with those of studies on immunization with vaccines based on TBEV-Eu or TBEV-FE which induced the production of cross-subtype reactive antibodies (Fritz et al., 2012; Domnich et al., 2014; Morozova et al., 2014; Chernokhaeva et al., 2016; Mcauley et al., 2017).

In this study, the mice were challenged with a lethal dose of TBEV, and a high level of viremia was observed on 3 dpi. The viremic phase was followed by the entry of the virus into the brain and intestinal tissues, which was consistent with the results of previous studies (Růžek et al., 2011; Palus et al., 2013). Importantly, the body weights of the immunized mice did not decrease and the mice survived the challenge, and the viral load in the sera and tissues was significantly lower than that of the non-immunized mice. Further histopathological analysis revealed the presence of obvious neuronal lesions and abnormal intestinal morphological structure in the control mice, while the mice in the VLP group exhibited normal form of organization. TBEV infection primarily target neurons, and cause neuronal damage and death (Mandl, 2005). Our murine model of TBE recapitulates the pathogenesis observed in previous studies (Palus et al., 2013).

The levels of various chemokines, colony-stimulating factors, and pro-inflammatory cytokines increase in the brain tissues of TBEV-infected mice (Pokorna Formanova et al., 2019). Analysis of the inflammatory cytokines in the brain tissues of mice following TBEV challenge revealed that CXCL10 was the most robustly upregulated chemokine in the brain. It has been reported that CXCL10 plays important roles in the recruitment of T cells expressing CXCR3 to the brain (Lepej et al., 2007; Groom and Luster, 2011; Pokorna Formanova et al., 2019); However, excessively high levels of CXCL10 in the central nervous system (CNS) can be harmful to the host (Sui et al., 2004, 2006). CXCL10 can cause pathological alterations via the excessive recruitment of cytotoxic T cells, and via its cytotoxic effects on neurons (Van Marle et al., 2004). Other studies have reported that the levels of CXCL10 are higher in the brain tissues of TBEV-infected mice at the time of viremia and viral neuro invasion (Pokorna Formanova et al., 2019). Increased levels of CXCL10 have also been detected in the cerebrospinal fluid (CSF) of humans infected with TBEV (Lepej et al., 2007; Zajkowska et al., 2011). It has also reported that the level of RANTES is higher in the CSF of TBE patients (Grygorczuk et al., 2006, 2018). Our findings are consistent with the results of these studies. The RANTES-mediated migration of monocytes and T lymphocytes in the blood may contribute to brain damage during TBEV infection (Zheng et al., 2018). We also revealed that the production of several key pro-inflammatory cytokines and chemokines, including MCP-1, MIP-1α, MIP-1β, and CXCL1 were upregulated following TBEV infection. The increased production of pro-inflammatory factors may mediate neuronal necrosis during the pathogenesis of TBEV. The expression of cytokines was undetectable in the immunized mice, which suggested that the VLPs alleviated the aggravated immune response induced by TBEV infection.

T cell responses are essential for the production of NAbs. Specific peptides of TBEV Core and E protein dominated the $CD4^+$ T cell response in both vaccinated and infected individuals (Kubinski et al., 2020). Various novel candidate flaviviral vaccines have been evaluated for their ability to enhance immunity by inducing virus-specific T cell responses. A previous study comparing the $CD4^+$ T cell responses in mice induced by rVSV encoding the ZIKV prM-E alone or together with the NS1 protein revealed that the co-expression of NS1 increased the $CD4^+$ IFN-γ^+ T cell response and decreased the population of $CD4^+$ TNF-α^+ Th1 cells (Li et al., 2018). Aberle et al. determined the levels of Th1-specific cytokines (TNF-α^+, IL-2^+, and IFN-γ^+), CD40 ligand, and the Th1 lineage-specifying transcription factor (Tbet) following stimulation with peptides targeting the structural proteins (C, prM/M, and E) of TBEV in the developed TBEV vaccine (Aberle et al., 2015). A similar approach was employed in this study, and the findings revealed that the levels of multiple-cytokine-producing antiviral $CD4^+$ T cells producing TNF-α^+, IL-2^+, or IFN-γ^+, increased in the immunized mice. Multi-cytokine-producing cells are more effective at controlling viral infection than single-cytokine producers (Makedonas and Betts, 2006; Pantaleo and Harari, 2006; Kannanganat et al., 2007; Wilkinson et al., 2012). These polyfunctional cells are possibly crucial for combating acute viral infection by producing high amounts of IFN-γ^+, and therefore contribute to the immediate effector function of T cells (Darrah et al., 2007; Weaver et al., 2013). The VLP vaccine developed in this study could possibly elicit the T cell response, which may play a crucial role in combating acute viral infection. However, TBEV-specific $CD4^+$ T cell responses are polyfunctional, while the cytokine patterns after vaccination with TBEV structure proteins were differed from those after TBEV infection, mainly reflected in IFN-γ responses and proportions of TNF-α^+IL-2^+ cells (Aberle et al., 2015). Thus, the assessment of $CD4^+$ T cell responses in VLP-immunized mice after TBEV infection is also worthy of further study to comprehensive analyze the T cell response of the VLPs-based vaccine.

Our study also has some limitations. VLPs generated in this study induced a T-cell mediated response, however, specific IgG subclasses in the serum was not detected. Generally, immunizations lead to memory B-cell activation and promoted the Th1-dominated immune response switch to a more balanced Th1/Th2 immune response. Additional studies should identify the role of these T cells, for example, the levels of both IgG2a and IgG1 isotypes. Furthermore, evidence for antibody-dependent enhancement (ADE) of TBEV *in vivo* is lacking so far, whereas the potential risk of enhanced infectivity should be taken into consideration in the development of novel vaccines. The protective immunity of the VLPs *in vivo* and the potential of the VLPs to induce ADE will be further investigated in *IFNAR*$^{-/-}$ mice.

5. Conclusions

Taken together, we described the efficient construction of TBE VLPs by plasmid-driven transfection of viral proteins in mammalian cells. Vaccination with VLPs induces a neutralizing-antibody response, stimulates multiple-cytokine-producing antiviral $CD4^+$ T cell response, and protects mice against lethal TBEV infection. We propose that TBEV VLPs should be further developed as a safe and effective vaccine candidate to protect humans against TBEV outbreaks.

Data availability

All data relevant to the study are included in the article or uploaded as supplementary information.

Ethics statement

All experiments involving the use of mice were approved by the Institutional Animal Care and Use Committee (IACUC) of the Wuhan Institute of Virology, Chinese Academy of Sciences (ethics number: WIVA02202004). The experiments were performed in accordance with the ABSL-3, National Biosafety Laboratory (Wuhan), Chinese Academy of Sciences guidelines and basic principles.

Author contributions

Jielin Tang: methodology, validation, investigation, data curation, formal analysis, visualization, writing-original draft, writing-reviewing, and editing. Muqing Fu: formal analysis, visualization, writing-original draft, writing-reviewing, and editing. Chonghui Xu: methodology, data curation. Bao Xue: investigation, formal analysis, data curation. Anqi Zhou: investigation. Sijie Chen: investigation. He Zhao: investigation. Yuan Zhou: supervision. Jizheng Chen: resources, formal analysis. Qi Yang: conceptualization, investigation, data curation, formal analysis, funding acquisition, methodology, validation, writing-original draft, writing-reviewing, and editing. Xinwen Chen: conceptualization, data curation, formal analysis, funding acquisition, supervision, validation, writing-reviewing, and editing.

Conflict of interest

The authors declare that the research was conducted in the absence of any commercial or financial relationships that could be construed as a potential conflict of interest. Prof. Xinwen Chen is an editorial board member for *Virologica Sinica*, and was not involved in the editorial review or the decision to publish this article.

Acknowledgements

This work was supported by grants from the National Key Research and Development Program of China (grant number: 2018YFA0507201 to X.W.C.), the National Science Foundation of China (grant number: 32000111 to Q.Y.), and the China Postdoctoral Science Foundation (grant number: 2020T130021ZX to Q.Y. and grant number: 2020M672580 to Q.Y.).

The authors acknowledge the National Virus Resource Center (NVRC, China) and the Center for Biosafety Mega-Science for providing the TBEV strains and usage of the BSL-3 laboratory. The authors thank F. X. Heinz for providing the TBEV strain. The authors express their gratitude to X. F. An and F. Zhang for their help with the animal experiments. The authors are grateful to P. Zhang, J. Wu, and J. Liu for advice and assistance during the manuscript preparation process.

Appendix A. Supplementary data

Supplementary data to this article can be found online at https://doi.org/10.1016/j.virs.2023.06.003.

References

Aberle, J.H., Aberle, S.W., Allison, S.L., Stiasny, K., Ecker, M., Mandl, C.W., Berger, R., Heinz, F.X., 1999. A DNA immunization model study with constructs expressing the tick-borne encephalitis virus envelope protein E in different physical forms. J. Immunol. 163, 6756–6761.

Aberle, J.H., Schwaiger, J., Aberle, S.W., Stiasny, K., Scheinost, O., Kundi, M., Chmelik, V., Heinz, F.X., 2015. Human CD4+ T helper cell responses after tick-borne encephalitis vaccination and infection. PLoS One 10, e0140545.

Bogovic, P., Strle, F., 2015. Tick-borne encephalitis: a review of epidemiology, clinical characteristics, and management. World J Clin Cases 3, 430–441.

Boigard, H., Alimova, A., Martin, G.R., Katz, A., Gottlieb, P., Galarza, J.M., 2017. Zika virus-like particle (VLP) based vaccine. PLoS Neglected Trop. Dis. 11, e0005608.

Chen, Q., Lai, H., 2013. Plant-derived virus-like particles as vaccines. Hum. Vaccines Immunother. 9, 26–49.

Chernokhaeva, L.L., Rogova, Y.V., Vorovitch, M.F., Romanova, L., Kozlovskaya, L.I., Maikova, G.B., Kholodilov, I.S., Karganova, G.G., 2016. Protective immunity spectrum induced by immunization with a vaccine from the TBEV strain Sofjin. Vaccine 34, 2354–2361.

Dai, L., Song, J., Lu, X., Deng, Y.Q., Musyoki, A.M., Cheng, H., Zhang, Y., Yuan, Y., Song, H., Haywood, J., Xiao, H., Yan, J., Shi, Y., Qin, C.F., Qi, J., Gao, G.F., 2016. Structures of the Zika virus envelope protein and its complex with a flavivirus broadly protective antibody. Cell Host Microbe 19, 696–704.

Darrah, P.A., Patel, D.T., De Luca, P.M., Lindsay, R.W., Davey, D.F., Flynn, B.J., Hoff, S.T., Andersen, P., Reed, S.G., Morris, S.L., Roederer, M., Seder, R.A., 2007. Multifunctional TH1 cells define a correlate of vaccine-mediated protection against Leishmania major. Nat. Med. 13, 843–850.

Demicheli, V., Debalini, M.G., Rivetti, A., 2009. Vaccines for Preventing Tick-Borne Encephalitis. Cochrane Database Syst Rev, p. Cd000977, 2009.

Domnich, A., Panatto, D., Arbuzova, E.K., Signori, A., Avio, U., Gasparini, R., Amicizia, D., 2014. Immunogenicity against Far Eastern and Siberian subtypes of tick-borne encephalitis (TBE) virus elicited by the currently available vaccines based on the European subtype: systematic review and meta-analysis. Hum. Vaccines Immunother. 10, 2819–2833.

Füzik, T., Formanová, P., Růžek, D., Yoshii, K., Niedrig, M., Plevka, P., 2018. Structure of tick-borne encephalitis virus and its neutralization by a monoclonal antibody. Nat. Commun. 9, 436.

Fritz, R., Orlinger, K.K., Hofmeister, Y., Janecki, K., Traweger, A., Perez-Burgos, L., Barrett, P.N., Kreil, T.R., 2012. Quantitative comparison of the cross-protection induced by tick-borne encephalitis virus vaccines based on European and Far Eastern virus subtypes. Vaccine 30, 1165–1169.

Garg, H., Mehmetoglu-Gurbuz, T., Ruddy, G.M., Joshi, A., 2019. Capsid containing virus like particle vaccine against Zika virus made from a stable cell line. Vaccine 37, 7123–7131.

Garg, H., Sedano, M., Plata, G., Punke, E.B., Joshi, A., 2017. Development of virus-like-particle vaccine and reporter assay for Zika virus. J. Virol. 91, e00834.

Groom, J.R., Luster, A.D., 2011. CXCR3 in T cell function. Exp. Cell Res. 317, 620–631.

Grygorczuk, S., Czupryna, P., Pancewicz, S., Świerzbińska, R., Kondrusik, M., Dunaj, J., Zajkowska, J., Moniuszko-Malinowska, A., 2018. Intrathecal expression of IL-5 and humoral response in patients with tick-borne encephalitis. Ticks Tick Borne Dis 9, 896–911.

Grygorczuk, S., Zajkowska, J., Swierzbińska, R., Pancewicz, S., Kondrusik, M., Hermanowska-Szpakowicz, T., 2006. [Concentration of the beta-chemokine CCL5 (RANTES) in cerebrospinal fluid in patients with tick-borne encephalitis]. Neurol. Neurochir. Pol. 40, 106–111.

Heinz, F.X., Allison, S.L., Stiasny, K., Schalich, J., Holzmann, H., Mandl, C.W., Kunz, C., 1995. Recombinant and virion-derived soluble and particulate immunogens for vaccination against tick-borne encephalitis. Vaccine 13, 1636–1642.

Holzer, G.W., Remp, G., Antoine, G., Pfleiderer, M., Enzersberger, O.M., Emsenhuber, W., Hämmerle, T., Gruber, F., Urban, C., Falkner, F.G., Dorner, F., 1999. Highly efficient induction of protective immunity by a vaccinia virus vector defective in late gene expression. J. Virol. 73, 4536–4542.

Jeong, H., Seong, B.L., 2017. Exploiting virus-like particles as innovative vaccines against emerging viral infections. J. Microbiol. 55, 220–230.

Kannanganat, S., Ibegbu, C., Chennareddi, L., Robinson, H.L., Amara, R.R., 2007. Multiple-cytokine-producing antiviral CD4 T cells are functionally superior to single-cytokine-producing cells. J. Virol. 81, 8468–8476.

Kubinski, M., Beicht, J., Gerlach, T., Volz, A., Sutter, G., Rimmelzwaan, G.F., 2020. Tick-borne encephalitis virus: a quest for better vaccines against a virus on the rise. Vaccines 8, 451.

Kunze, U., 2011. Tick-borne encephalitis: the impact of epidemiology, changing lifestyle, and environmental factors. Conference report of the 12th annual meeting of the international scientific working group on tick-borne encephalitis (ISW-TBE). Vaccine 29, 1355–1356.

Lepej, S.Z., Misić-Majerus, L., Jeren, T., Rode, O.D., Remenar, A., Sporec, V., Vince, A., 2007. Chemokines CXCL10 and CXCL11 in the cerebrospinal fluid of patients with tick-borne encephalitis. Acta Neurol. Scand. 115, 109–114.

Li, P., Yao, C., Wang, T., Wu, T., Yi, W., Zheng, Y., Miao, Y., Sun, J., Tan, Z., Liu, Y., Zhang, X., Wang, H., Zheng, Z., 2021. Recovery of a Far-Eastern Strain of Tick-Borne Encephalitis Virus with a Full-Length Infectious cDNA Clone. Virol. Sin. 36, 1375–1386.

Li, A., Yu, J., Lu, M., Ma, Y., Attia, Z., Shan, C., Xue, M., Liang, X., Craig, K., Makadiya, N., He, J.J., Jennings, R., Shi, P.Y., Peeples, M.E., Liu, S.L., Boyaka, P.N., Li, J., 2018. A Zika virus vaccine expressing premembrane-envelope-NS1 polyprotein. Nat. Commun. 9, 3067.

Lin, H.H., Yip, B.S., Huang, L.M., Wu, S.C., 2018. Zika virus structural biology and progress in vaccine development. Biotechnol. Adv. 36, 47–53.

Lindquist, L., Vapalahti, O., 2008. Tick-borne encephalitis. Lancet 371, 1861–1871.

Liu, Y., Zhou, J., Yu, Z., Fang, D., Fu, C., Zhu, X., He, Z., Yan, H., Jiang, L., 2014. Tetravalent recombinant dengue virus-like particles as potential vaccine candidates: immunological properties. BMC Microbiol. 14, 233.

Liu, Y.L., Si, B.Y., Hu, Y., Zhang, Y., Yang, Y.H., Zhu, Q.Y., 2005. [Expression of tick-borne encephalitis virus prM-E protein in insect cells and studies on its antigenicity]. Zhonghua Shi Yan He Lin Chuang Bing Du Xue Za Zhi 19, 335–339.

Lobigs, M., 1993. Flavivirus premembrane protein cleavage and spike heterodimer secretion require the function of the viral proteinase NS3. Proc. Natl. Acad. Sci. U. S. A. 90, 6218–6222.
Loew-Baselli, A., Konior, R., Pavlova, B.G., Fritsch, S., Poellabauer, E., Maritsch, F., Harmacek, P., Krammer, M., Barrett, P.N., Ehrlich, H.J., 2006. Safety and immunogenicity of the modified adult tick-borne encephalitis vaccine FSME-IMMUN: results of two large phase 3 clinical studies. Vaccine 24, 5256–5263.
Makedonas, G., Betts, M.R., 2006. Polyfunctional Analysis of Human T Cell Responses: Importance in Vaccine Immunogenicity and Natural Infection. Springer Semin Immunopathol 28, 209–219.
Malogolovkin, A., Davies, A., Abouelhadid, S., Kerviel, A., Roy, P., Falconar, A.K., 2023. Enhanced Zika virus-like particle development using Baculovirus spp. constructs. J. Med. Virol. 95, e28252.
Mandl, C.W., 2005. Steps of the tick-borne encephalitis virus replication cycle that affect neuropathogenesis. Virus Res. 111, 161–174.
Mcauley, A.J., Sawatsky, B., Ksiazek, T., Torres, M., Korva, M., Lotrič-Furlan, S., Avšič-Županc, T., Von Messling, V., Holbrook, M.R., Freiberg, A.N., Beasley, D.W.C., Bente, D.A., 2017. Cross-neutralisation of viruses of the tick-borne encephalitis complex following tick-borne encephalitis vaccination and/or infection. NPJ Vaccines 2, 5.
Metz, S.W., Thomas, A., White, L., Stoops, M., Corten, M., Hannemann, H., De Silva, A.M., 2018. Dengue virus-like particles mimic the antigenic properties of the infectious dengue virus envelope. Virol. J. 15, 60.
Morozova, O.V., Bakhvalova, V.N., Potapova, O.F., Grishechkin, A.E., Isaeva, E.I., Aldarov, K.V., Klinov, D.V., Vorovich, M.F., 2014. Evaluation of immune response and protective effect of four vaccines against the tick-borne encephalitis virus. Vaccine 32, 3101–3106.
Palus, M., Vojtíšková, J., Salát, J., Kopecký, J., Grubhoffer, L., Lipoldová, M., Demant, P., Růžek, D., 2013. Mice with different susceptibility to tick-borne encephalitis virus infection show selective neutralizing antibody response and inflammatory reaction in the central nervous system. J. Neuroinflammation 10, 77.
Pantaleo, G., Harari, A., 2006. Functional signatures in antiviral T-cell immunity for monitoring virus-associated diseases. Nat. Rev. Immunol. 6, 417–423.
Phanthanawiboon, S., Limkittikul, K., Sakai, Y., Takakura, N., Saijo, M., Kurosu, T., 2016. Acute systemic infection with dengue virus leads to vascular leakage and death through tumor necrosis factor-α and tie2/angiopoietin signaling in mice lacking type I and II interferon receptors. PLoS One 11, e0148564.
Pokorna Formanova, P., Palus, M., Salat, J., Hönig, V., Stefanik, M., Svoboda, P., Ruzek, D., 2019. Changes in cytokine and chemokine profiles in mouse serum and brain, and in human neural cells, upon tick-borne encephalitis virus infection. J. Neuroinflammation 16, 205.
Pulkkinen, L.I.A., Butcher, S.J., Anastasina, M., 2018. Tick-borne encephalitis virus: a structural view. Viruses 10, 350–370.
Ruzek, D., Avšič Županc, T., Borde, J., Chrdle, A., Eyer, L., Karganova, G., Kholodilov, I., Knap, N., Kozlovskaya, L., Matveev, A., Miller, A.D., Osolodkin, D.I., verby, A.K., Tikunova, N., Tkachev, S., Zajkowska, J., 2019. Tick-borne encephalitis in Europe and Russia: review of pathogenesis, clinical features, therapy, and vaccines. Antivir. Res. 164, 23–51.
Růžek, D., Salát, J., Singh, S.K., Kopecký, J., 2011. Breakdown of the blood-brain barrier during tick-borne encephalitis in mice is not dependent on CD8+ T-cells. PLoS One 6, e20472.
Stocks, C.E., Lobigs, M., 1998. Signal peptidase cleavage at the flavivirus C-prM junction: dependence on the viral NS2B-3 protease for efficient processing requires determinants in C, the signal peptide, and prM. J. Virol. 72, 2141–2149.
Studahl, M., Lindquist, L., Eriksson, B.M., Günther, G., Bengner, M., Franzen-Röhl, E., Fohlman, J., Bergström, T., Aurelius, E., 2013. Acute viral infections of the central nervous system in immunocompetent adults: diagnosis and management. Drugs 73, 131–158.
Sui, Y., Potula, R., Dhillon, N., Pinson, D., Li, S., Nath, A., Anderson, C., Turchan, J., Kolson, D., Narayan, O., Buch, S., 2004. Neuronal apoptosis is mediated by CXCL10 overexpression in simian human immunodeficiency virus encephalitis. Am. J. Pathol. 164, 1557–1566.
Sui, Y., Stehno-Bittel, L., Li, S., Loganathan, R., Dhillon, N.K., Pinson, D., Nath, A., Kolson, D., Narayan, O., Buch, S., 2006. CXCL10-induced cell death in neurons: role of calcium dysregulation. Eur. J. Neurosci. 23, 957–964.
Suss, J., 2008. Tick-borne encephalitis in Europe and beyond–the epidemiological situation as of 2007. Euro Surveill. 13, 18916–18924.
Taba, P., Schmutzhard, E., Forsberg, P., Lutsar, I., Ljøstad, U., Mygland, Levchenko, I., Strle, F., Steiner, I., 2017. EAN consensus review on prevention, diagnosis and management of tick-borne encephalitis. Eur. J. Neurol. 24, 1214–1261.
Tang, J., Xu, C., Fu, M., Liu, C., Zhang, X., Zhang, W., Pei, R., Wang, Y., Zhou, Y., Chen, J., Miao, Z., Pan, G., Yang, Q., Chen, X., 2023. Sterile 20-like kinase 3 promotes tick-borne encephalitis virus assembly by interacting with NS2A and prM and enhancing the NS2A-NS4A association. J. Med. Virol. https://doi.org/10.1002/jmv.28610.
Taylor, T.J., Diaz, F., Colgrove, R.C., Bernard, K.A., Deluca, N.A., Whelan, S.P.J., Knipe, D.M., 2016. Production of immunogenic West Nile virus-like particles using a herpes simplex virus 1 recombinant vector. Virology 496, 186–193.
Urakami, A., Ngwe Tun, M.M., Moi, M.L., Sakurai, A., Ishikawa, M., Kuno, S., Ueno, R., Morita, K., Akahata, W., 2017. An envelope-modified tetravalent dengue virus-like-particle vaccine has implications for flavivirus vaccine design. J. Virol. 91, e01181.
Van Marle, G., Henry, S., Todoruk, T., Sullivan, A., Silva, C., Rourke, S.B., Holden, J., Mcarthur, J.C., Gill, M.J., Power, C., 2004. Human immunodeficiency virus type 1 Nef protein mediates neural cell death: a neurotoxic role for IP-10. Virology 329, 302–318.
Vang, L., Morello, C.S., Mendy, J., Thompson, D., Manayani, D., Guenther, B., Julander, J., Sanford, D., Jain, A., Patel, A., Shabram, P., Smith, J., Alexander, J., 2021. Zika virus-like particle vaccine protects AG129 mice and rhesus macaques against Zika virus. PLoS Neglected Trop. Dis. 15, e0009195.
Weaver, J.M., Yang, H., Roumanes, D., Lee, F.E., Wu, H., Treanor, J.J., Mosmann, T.R., 2013. Increase in IFNγ(-)IL-2(+) cells in recent human CD4 T cell responses to 2009 pandemic H1N1 influenza. PLoS One 8, e57275.
Werme, K., Wigerius, M., Johansson, M., 2008. Tick-borne encephalitis virus NS5 associates with membrane protein scribble and impairs interferon-stimulated JAK-STAT signalling. Cell Microbiol. 10, 696–712.
Wilkinson, T.M., Li, C.K., Chui, C.S., Huang, A.K., Perkins, M., Liebner, J.C., Lambkin-Williams, R., Gilbert, A., Oxford, J., Nicholas, B., Staples, K.J., Dong, T., Douek, D.C., Mcmichael, A.J., Xu, X.N., 2012. Preexisting influenza-specific CD4+ T cells correlate with disease protection against influenza challenge in humans. Nat. Med. 18, 274–280.
Yamaji, H., Konishi, E., 2016. Production of Japanese encephalitis virus-like particles using insect cell expression systems. Methods Mol. Biol. 1404, 365–375.
Yang, L., Xiao, A., Wang, H., Zhang, X., Zhang, Y., Li, Y., Wei, Y., Liu, W., Chen, C., 2022. A VLP-Based Vaccine Candidate Protects Mice against Japanese Encephalitis Virus Infection. Vaccines, Basel, p. 10.
Yang, Q., Pei, R., Wang, Y., Zhou, Y., Yang, M., Chen, X., Chen, J., 2021. ADAM15 participates in tick-borne encephalitis virus replication. J. Virol. 95, e01926-e01946.
Yang, Q., You, J., Zhou, Y., Wang, Y., Pei, R., Chen, X., Yang, M., Chen, J., 2020. Tick-borne encephalitis virus NS4A ubiquitination antagonizes type I interferon-stimulated STAT1/2 signalling pathway. Emerg. Microb. Infect. 9, 714–726.
Zajkowska, J., Moniuszko-Malinowska, A., Pancewicz, S.A., Muszyńska-Mazur, A., Kondrusik, M., Grygorczuk, S., Swierzbińska-Pijanowska, R., Dunaj, J., Czupryna, P., 2011. Evaluation of CXCL10, CXCL11, CXCL12 and CXCL13 chemokines in serum and cerebrospinal fluid in patients with tick borne encephalitis (TBE). Adv. Med. Sci. 56, 311–317.
Zhao, Z., Deng, Y., Niu, P., Song, J., Wang, W., Du, Y., Huang, B., Wang, W., Zhang, L., Zhao, P., Tan, W., 2021. Co-immunization with CHIKV VLP and DNA vaccines induces a promising humoral response in mice. Front. Immunol. 12, 655743.
Zheng, Z., Yang, J., Jiang, X., Liu, Y., Zhang, X., Li, M., Zhang, M., Fu, M., Hu, K., Wang, H., Luo, M.H., Gong, P., Hu, Q., 2018. Tick-borne encephalitis virus nonstructural protein NS5 induces RANTES expression dependent on the RNA-dependent RNA polymerase activity. J. Immunol. 201, 53–68.